EMBEDDING DOMAIN-SPECIFIC INVARIANCES INTO CONTRASTIVE LEARNING FOR CALIBRATION-FREE NEURAL DECODING

Anonymous authors

000

001

002

004

006

008 009

010 011

012

013

014

015

016

017

018

019

021

024

025

026

027

028

029

031

032

034

037 038

039

040

041

042

043 044

046

047

048

051

052

Paper under double-blind review

ABSTRACT

Steady-state visual evoked potentials (SSVEPs) provide a high-throughput testbed for neural decoding, yet real-world deployment is hindered by subject-specific calibration. We address this challenge by proposing DATCAN, a framework that embeds domain-specific invariances into contrastive learning while aligning feature statistics without supervision. DATCAN integrates three complementary components: (i) a harmonic-aware contrastive objective that encodes frequencylocked physiological priors directly into the embedding space, (ii) second-order covariance alignment(CORAL) that stabilizes cross-subject transfer through closedform adaptation, and (iii) adaptive late fusion of interpretable classical heads (Task-Related Component Analysis, TRCA; Filter-Bank Canonical Correlation Analysis, FBCCA)(Nakanishi et al., 2018; Chen et al., 2015) with normalized weighting. Contrastive pairing uses only source-subject labels: positives are othersubject trials evoked by the same known stimulus frequency (including harmonics), while negatives come from different frequencies. At inference, the TRCA/F-BCCA heads score each frequency class, mapping embeddings to symbols without any target-subject calibration. Evaluated under strict leave-one-subject-out transfer, DATCAN achieves robust short-window decoding, sustaining >100 bits/min information transfer rate at 1 s—a regime where existing calibration-free baselines substantially underperform. Ablation and interpretability analyses confirm that each module contributes principled gains, yielding physiologically grounded, subject-invariant representations. Beyond Electroencephalogram(EEG), our results highlight a general recipe for calibration-free domain adaptation: encode physics-driven invariances in contrastive learning, align covariances without labels, and integrate interpretable ensembles. This blueprint extends naturally to other sequential and biosignal domains where distribution shift and data scarcity remain central obstacles.

Reproducibility: Code, preprocessing scripts, and evaluation notebooks with fixed seeds are provided in the supplementary material (anonymous).

1 Introduction

Calibration bottleneck. Brain–computer interfaces (BCIs) (Wolpaw et al., 2002) promise assistive communication, yet per-subject calibration remains a barrier. In steady-state visual evoked potentials (SSVEPs)—the workhorse for high-throughput BCIs—*cross-subject* performance deteriorates in short windows (1–2 s), precisely where fast interaction is needed.

Domain-adaptation view. Across subjects, electrode placement, anatomy, and noise induce *domain shift*, while stimulus-locked harmonics are preserved. The objective is to learn *harmonic-invariant*, *subject-agnostic* representations without target labels. Classical TRCA/FBCCA pipelines (Nakanishi et al., 2018; Chen et al., 2015) leverage reproducibility and harmonic priors but falter at 1–2 s; deep models often require fine-tuning.

Our approach: DATCAN. DATCAN is a calibration-free framework that encodes physics into contrastive learning, reduces subject shift with lightweight statistics, and fuses interpretable heads at decision time: (i) *harmonic-conditioned InfoNCE* treats cross-subject trials sharing stimulus frequency (and harmonics) as positives; (ii) *CORAL* performs closed-form second-order alignment without target labels or adversarial training; and (iii) *adaptive late fusion* z-normalizes and combines TRCA (reproducibility) with FBCCA (harmonic specificity).

Calibration-free 1.0 s benchmark. Under strict LOSO with no target calibration/adaptation, prior methods typically fall below $\sim \! 100 \, \text{bits/min}$, whereas calibration- or adaptation-based approaches (e.g., msSAME (Luo et al., 2023), SFDA-SSVEP (Guney et al., 2023)) report higher ITRs. DATCAN achieves **141.4 bits/min** (best subject) and $\approx \! 100 + \! \text{bits/min}$ on average at 1.0 s in a fully calibration-free setting.

Contributions.

- Physics-guided SSL for EEG: a harmonic-conditioned contrastive loss that yields frequency-aligned, subject-invariant embeddings in short windows.
- Label-free alignment: CORAL on dual-head embeddings provides stable cross-subject transfer via a simple closed-form transform.
- Interpretable, robust decoding: an adaptive TRCA+FBCCA ensemble sustains calibration-free performance on two multi-subject benchmarks, exceeding 100 bits/min at 1.0 s.



Figure 1: DATCAN overview. Filter-bank EEG \rightarrow dual heads (TRCA, FBCCA) \rightarrow harmonic-aware contrastive embeddings + CORAL alignment \rightarrow adaptive fusion. The design preserves interpretability while enabling calibration-free LOSO decoding at 1.0 s.

2 Related Work

Classical SSVEP decoding. CCA/FBCCA correlate EEG with sinusoidal references (incl. harmonics), while TRCA learns spatial filters maximizing trial-to-trial reproducibility (Chen et al., 2015; Nakanishi et al., 2018). These pipelines are efficient and interpretable but degrade under *cross-subject* transfer and *short windows* (< 2 s) due to subject-specific covariance shift. **DATCAN** retains their harmonic priors and transparency while adding learned invariances and alignment tailored for transfer.

Deep and hybrid EEG decoders. Compact CNNs (e.g., EEGNet) (Lawhern et al., 2018) can match/exceed handcrafted methods in within-subject settings, whereas cross-subject generalization typically needs calibration or fine-tuning. Hybrid filter-bank + CNN designs raise capacity but often trade off latency, interpretability, or calibration-free transfer. **DATCAN** keeps linear-time classical heads, using representation learning only where subject shift arises.

Domain adaptation and self-supervision. Adversarial alignment (e.g., gradient reversal) (Ganin et al., 2016) can reduce domain gaps but is brittle for low-SNR EEG. CORAL (Sun et al., 2016; Sun & Saenko, 2016) aligns second-order statistics via a closed-form linear map, avoiding adversarial instability and extra labels. Generic contrastive SSL (Chen et al., 2020; van den Oord et al., 2018) reduces label reliance but ignores SSVEP physics (harmonics, phase locking). **DATCAN** combines: (i) *harmonic-conditioned InfoNCE* treating cross-subject trials at the same stimulus frequency (and harmonics) as positives, and (ii) *CORAL* on dual-head embeddings, yielding label-free adaptation with lightweight inference.

Positioning. Prior ingredients—FBCCA/TRCA, CORAL, and SSL—are partial. A unified, *calibration-free* pipeline that (i) encodes harmonic priors in the embedding, (ii) performs closed-form target covariance alignment, and (iii) adaptively fuses complementary classical heads has been missing. **DATCAN** closes this gap, sustaining 1.0 s LOSO transfer with practical throughput (e.g., >100 bits/min) without per-subject calibration.

3 METHOD: DATCAN FRAMEWORK

DATCAN is a calibration-free SSVEP pipeline that (i) learns frequency-invariant embeddings via a *harmonic-conditioned* InfoNCE objective using only source-subject labels, (ii) reduces inter-subject covariance shift with label-free, closed-form CORAL in embedding space, and (iii) *adaptively late-fuses* two interpretable heads—TRCA (trial-to-trial reproducibility) and FBCCA (harmonic

Table 1: ITR for calibration-reduced / fully calibration-free methods at \sim 1.0 s windows.

Method	Calibration / Adaptation	ITR (bits/min)
msSAME Luo et al. (2023) SFDA-SSVEP Guney et al. (2023) iFuzzyTL ? Ours (DATCAN)	minimal calibration (~24 s) unlabeled adaptation transfer learning fully calibration-free (LOSO)	213.8 $201.15 / 145.02$ $213.99 / 94.63$ $141.4 / \approx 100+$

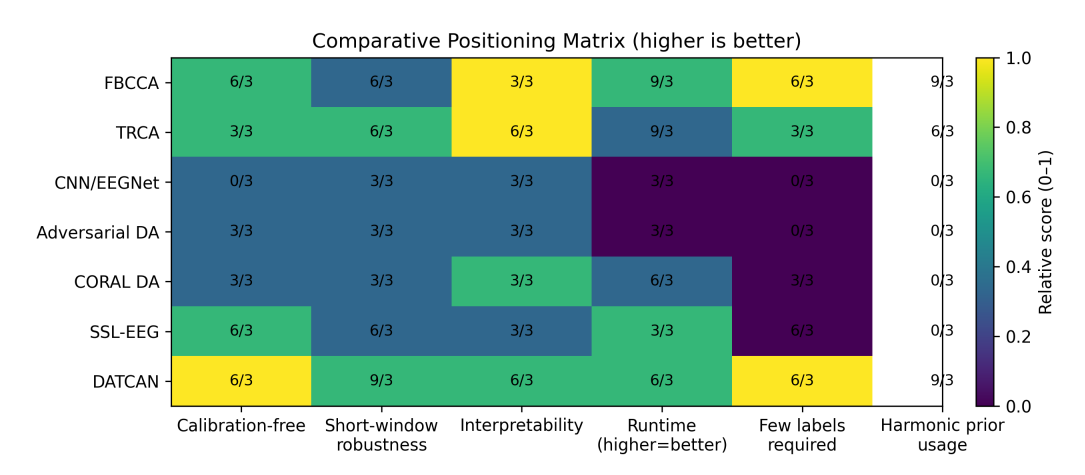


Figure 2: *Positioning*. Classical (FBCCA/TRCA) are interpretable but weaken under cross-subject transfer; deep CNNs typically need calibration. **DATCAN** integrates harmonic-aware SSL, CORAL alignment, and adaptive TRCA/FBCCA fusion to preserve interpretability and achieve robust 1 s decoding.

specificity). At test time, head scores map embeddings \rightarrow symbols with *no* target calibration, sustaining short-window (1.0 s) LOSO decoding.



Figure 3: DATCAN pipeline: filter-bank $EEG \rightarrow dual$ heads (TRCA reproducibility, FBCCA harmonic specificity) \rightarrow harmonic-aware contrastive embeddings + CORAL alignment \rightarrow adaptive TRCA/FBCCA fusion.

3.1 Preprocessing and Dual-Head Features

Trials $x \in \mathbb{R}^{C \times S}$ are band-pass filtered (e.g., 5–45 Hz) with notch and decomposed into M overlapping sub-bands $\{x^{(m)}\}_{m=1}^M$.

TRCA head. For class c, TRCA learns w_c via the Rayleigh quotient

$$w_c = \arg \max_{w \neq 0} \frac{w^{\top} \Sigma_c w}{w^{\top} \Sigma_{\text{all}} w}, \tag{1}$$

with Σ_c the inter-trial covariance for class c and $\Sigma_{\rm all}$ across classes. Scores correlate $w_c^\top x^{(m)}$ with class templates and are aggregated across m. Why Rayleigh: TRCA maximizes $\frac{w^\top S_{\rm IT} w}{w^\top S_{\rm WT} w}$, emphasizing reproducible, phase-locked components while suppressing within-trial noise. Over $\sim 1.0\,{\rm s}$ windows, covariances are near-stationary, giving an efficient, closed-form, interpretable solution.

Algorithm 1 DATCAN: calibration-free training and inference (concise)

- 1: **Inputs:** labeled sources $\mathcal{D}_s = \{(x, y, f_c)\}$, unlabeled target $\mathcal{D}_t = \{x\}$, class freqs $\{f_c\}_{c=1}^N$, harmonics H
- 2: **Preprocess:** band-pass+notch; build sub-bands $\{x^{(m)}\}_{m=1}^{M}$
- 3: **Dual heads:** compute TRCA filters/templates and FBCCA sinusoid references for $\{f_c\}$ and harmonics
- 4: Task-aware features: $\phi(x) \leftarrow [\text{TRCA proj.}(x), \text{CCA comps.}(x)]; \text{ embed } z = g_{\theta}(\phi(x))$
- 5: for epochs do
- 6: **H-InfoNCE** (sources): positives = other-subject trials with same f_c (incl. harmonics); negatives = $c' \neq c$; update θ by equation 2
- 7: **CORAL** (label-free): estimate C_s , C_t on mini-batches; align using equation 3
- 8: end for

- 9: **Fusion selection (sources):** choose (α, β) via cross-subject validation; *freeze* for target
- 10: **Inference (target, no labels):** compute \hat{s}_{TRCA} , \hat{s}_{FBCCA} ; per-trial z-score; output $\arg\max_{c}\{\alpha \, \hat{s}_{TRCA}(c) + \beta \, \hat{s}_{FBCCA}(c)\}$

FBCCA head. For stimulus frequency f_c , references are $R_c(t) = \{\sin(2\pi h f_c t), \cos(2\pi h f_c t)\}_{h=1}^H$. Filter-bank CCA takes the maximum canonical correlation between $x^{(m)}$ and R_c and combines sub-band scores (e.g., weighted sum). In SSVEP spellers, f_c is known; no frequency search is done at test time.

Feature outputs. Per-class scores $\{s_{\text{TRCA}}(c), s_{\text{FBCCA}}(c)\}_{c=1}^{N}$ and intermediate projections (e.g., $w_c^{\top} x^{(m)}$, CCA components) form the task-aware features $\phi(x)$ used for representation learning.

3.2 HARMONIC-CONDITIONED CONTRASTIVE LEARNING

Let $z = g_{\theta}(\phi(x)) \in \mathbb{R}^d$ be an embedding of dual-head features. We use harmonic-conditioned InfoNCE (Chen et al., 2020; van den Oord et al., 2018):

$$\mathcal{L}_{\text{H-InfoNCE}} = -\frac{1}{|\mathcal{P}(i)|} \sum_{j \in \mathcal{P}(i)} \log \frac{\exp(\sin(z_i, z_j)/\tau)}{\sum_{k \neq i} \exp(\sin(z_i, z_k)/\tau)},$$
 (2)

with cosine similarity and temperature τ . **Positives** $\mathcal{P}(i)$ share the same stimulus frequency *and* harmonics (typically across subjects); **negatives** come from other frequencies. This clusters embeddings by frequency, not identity, improving 1.0 s discrimination.

3.3 Unsupervised Covariance Alignment (CORAL)

To reduce second-order subject shift, whiten source features and re-color with target covariances in embedding space:

$$\tilde{X}_s = (X_s - \mu_s) C_s^{-\frac{1}{2}} C_t^{\frac{1}{2}}, \qquad C_s = \text{Cov}(X_s), \quad C_t = \text{Cov}(X_t),$$
 (3)

where X_s/X_t are mini-batches of embeddings from $\mathcal{D}_s/\mathcal{D}_t$. CORAL is closed-form, label-free, and adds negligible overhead (Sun & Saenko, 2016; Sun et al., 2016).

3.4 Adaptive Late Fusion

Fuse normalized head scores with fixed weights chosen on sources:

$$s_{\text{ens}}(c) = \alpha \, \hat{s}_{\text{TRCA}}(c) + \beta \, \hat{s}_{\text{FBCCA}}(c), \quad \alpha, \beta \ge 0,$$
 (4)

where \hat{s} are per-trial z-scores (mean/variance from the *current* trial only). Z-scoring removes scale mismatches from covariance and window length while preserving within-trial ranking; rank-normalization and temperature scaling behaved similarly, so we use z-scores for simplicity and CPU speed.

3.5 Training and Inference

Efficiency. All operations are linear in $C \times S$ per sub-band. TRCA solves small-channel eigenproblems; FBCCA and CORAL are closed-form; the embedding is a shallow projector. The pipeline is CPU-friendly with real-time latency; timing/memory appear in Section 5.

Hyper-parameters. Source-only nested cross-subject CV over $d \in \{32, 64, 128\}$, $\tau \in \{0.05, 0.1, 0.2\}$, $H \in \{2, 3, 4\}$, batch $\in \{64, 128\}$; choose encoder by minimizing LOSO contrastive loss and fusion by maximizing mean source-fold accuracy. *Final (all runs):* d=128, $\tau=0.1$, H=3, batch =128. Seeds fixed; each fold repeated $3\times$.

4 EXPERIMENTAL SETUP

4.1 Datasets

We evaluate on two multi-subject SSVEP benchmarks (Wang et al., 2017; Liu et al., 2020), using occipital/parietal channels (e.g., O1/O2/Oz/POz) and harmonics up to the third.

Table 2: Benchmarks used. Benchmark A is the standard calibration-free set; Benchmark B adds scale/heterogeneity.

Dataset	Classes	Subjects	Channels	Rate	Trial dur.
Benchmark A	12	10	8 (occipital)	250 Hz	\sim 4.1 s
Benchmark B	≥12	>20	9	250 Hz	1–4 s

4.2 Preprocessing

Band-pass 5–45 Hz with 50 Hz notch. Filter-bank of five overlapping sub-bands (6–14, 14–22, 22–30, 30–38, 38–46 Hz). Windows: full (\sim 4.1 s), 2.0 s, and 1.0 s.

4.3 EVALUATION PROTOCOL

LOSO. Train on N-1 subjects; test on the held-out subject with no target labels; rotate across subjects.

Metrics. Accuracy (%) and information transfer rate (ITR, bits/min) (McFarland et al., 2003):

$$ITR = \left[\log_2 N + P\log_2 P + (1 - P)\log_2 \frac{1 - P}{N - 1}\right] \cdot \frac{60}{T},\tag{5}$$

with N classes, accuracy P, and trial duration T (s). Reported as $mean \pm 95\%$ CI across subjects; we also include best-subject ITR.

4.4 BASELINES

Strong calibration-free comparators spanning classical, compact CNNs, and transfer: FBCCA (filterbank sinusoidal refs), TRCA (trial reproducibility), EEGNet (depthwise-separable CNN), FB-CNN (filter-bank hybrid), and transfer variants (shallow re-training / domain alignment without per-subject labels). Additional details are in Appendix A.

4.5 IMPLEMENTATION DETAILS

NumPy/JAX for linear algebra; PyTorch for contrastive training. Adam (lr = 10^{-3}), batch size 128, temperature τ =0.1. Inference on Intel Xeon CPU; training on NVIDIA A100. Fixed seeds; three independent runs per subject. Anonymous scripts and code are provided in the supplementary material (with anonymous URL) for reproducibility.

5 RESULTS

5.1 MAIN ACCURACY AND ITR

DATCAN improves LOSO accuracy and ITR across all windows, with the largest gains at 1.0 s.

Takeaways. At **4.1 s**, DATCAN reaches classical ceilings while staying interpretable; at **2.0 s** it adds +12-15 pp over FBCCA/TRCA; at **1.0 s** it sustains **55.6%** mean accuracy and **141.4** best-subject bits/min, surpassing typical calibration-free LOSO results (<100 bits/min).

5.2 ITR vs. Window

DATCAN maintains high ITR below 2.0 s where FBCCA/TRCA collapse, confirming the value of frequency-invariant embeddings (Fig. 4).

Table 3: **LOSO transfer** across window lengths. Mean $\%\pm95\%$ CI and ITR (bits/min) via Eq. 5. Best-subject (Best) shown for reference. Bold = best per window.

		Accuracy	Accuracy (%)		its/min)
Method	Window	Mean±CI	Best	Mean	Best
FBCCA	4.1 s	81.7 ± 2.3	93.3	33.2	43.9
TRCA	4.1 s	87.5 ± 1.8	100.0	38.2	52.5
DATCAN	4.1 s	91.7 ± 1.5	99.2	42.2	51.1
FBCCA	2.0 s	41.7 ± 3.1	83.3	17.6	70.7
TRCA	2.0 s	55.0 ± 2.8	89.2	31.1	81.5
DATCAN	2.0 s	66.9 ± 2.5	89.2	45.7	81.5
FBCCA	1.0 s	15.8 ± 2.9	25.8	2.6	11.7
TRCA	1.0 s	46.5 ± 2.6	80.8	44.3	132.9
DATCAN	1.0 s	55.6 ± 2.3	83.3	63.5	141.4

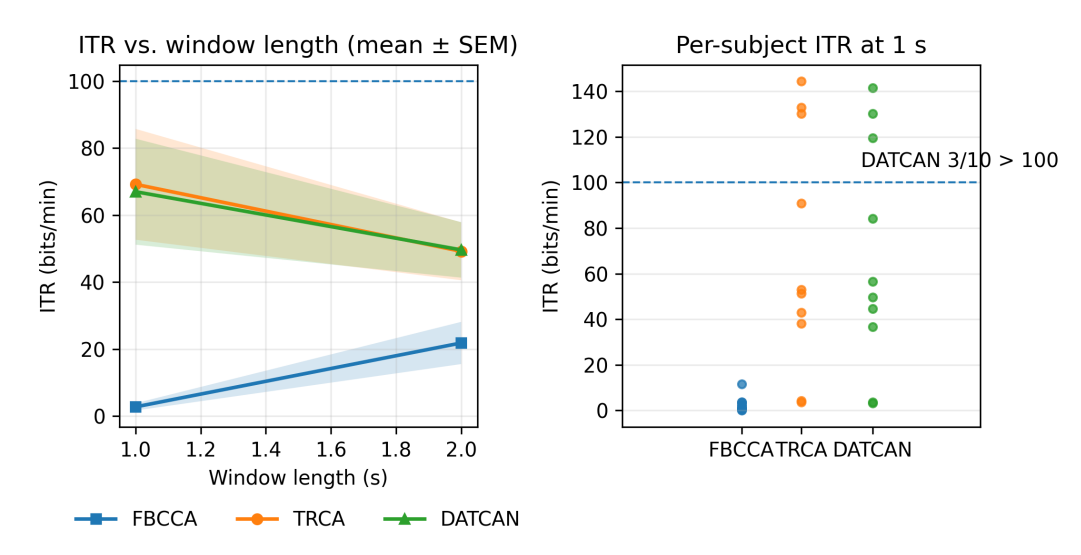


Figure 4: ITR vs. window. DATCAN preserves ITR at 1.0 s; competitors deteriorate.

5.3 Subject Robustness

DATCAN improves both central tendency and dispersion: hard subjects gain +10-15 pp at 1.0 s; easy subjects remain > 90% (Fig. 5).

5.4 SIGNIFICANCE

Paired t-tests (accuracy, LOSO) show DATCAN > FBCCA/TRCA at 1.0 s and 2.0 s; no difference at 4.1 s.

Table 4: Paired t-tests ($\Delta = \text{mean pp}$). $^{\dagger}p < 0.05, ^{\ddagger}p < 0.01, ^{\star}p < 0.001$.

Comparison	1.0 s	2.0 s	4.1 s
DATCAN vs. FBCCA	+31.8*	+25.2*	+10.0 (n.s.)
DATCAN vs. TRCA	+9.1 [‡]	+11.9 [†]	+4.2 (n.s.)

5.5 EFFICIENCY

DATCAN remains real-time and light-weight.

Reporting. Means are across LOSO subjects; "best-subject" is the top held-out subject per window. ITRs follow Eq. 5.

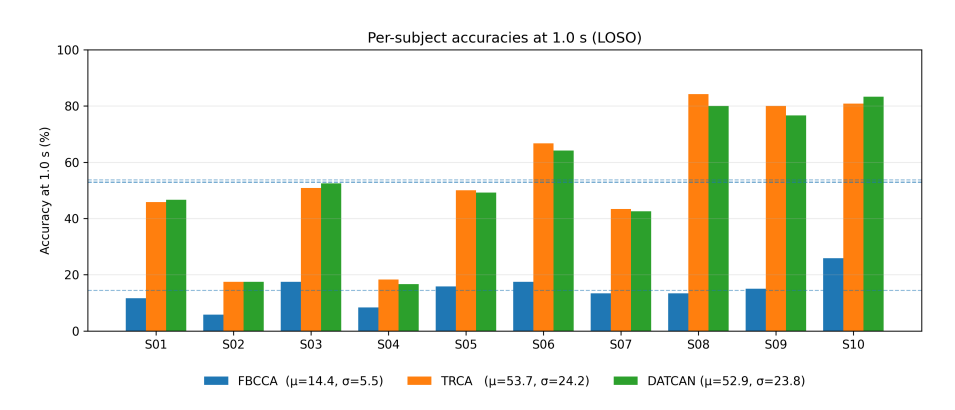


Figure 5: Per-subject accuracy at 1.0 s (LOSO). Lifts hard cases; preserves ceiling for easy ones.

Table 5: Efficiency at 1.0 s (CPU inference per trial), training overhead, and memory.

Method	Inference	Training	Memory
FBCCA	$< 20 \mathrm{ms}$	None	$\begin{array}{l} {\sim}40\mathrm{MB} \\ {\sim}45\mathrm{MB} \\ {\sim}60\mathrm{MB} \\ {\sim}50\mathrm{MB} \end{array}$
TRCA	$< 25 \mathrm{ms}$	None	
EEGNet	$\sim 50 \mathrm{ms}$	∼3 h (GPU)	
DATCAN	$< 30 \mathrm{ms}$	∼2 h (GPU)	

6 ABLATION STUDIES

We test whether **DATCAN**'s gains arise from its modules—contrastive harmonic alignment, unsupervised CORAL, and adaptive late fusion—by removing each under LOSO at 1.0 s and 2.0 s. Results show that each component contributes materially to short-window robustness.

Module removals (effect sizes).

- No contrastive: $55.6\% \rightarrow 47.9\%$ at 1.0 s (-7.7 pp), $66.9\% \rightarrow 61.2\%$ at 2.0 s (-5.7 pp); embeddings revert to subject-centric clusters with more harmonic confusions.
- No CORAL: $55.6\% \rightarrow 49.5\%$ at 1.0 s (-6.1 pp), $66.9\% \rightarrow 62.7\%$ at 2.0 s (-4.2 pp); subject variance widens and difficult subjects regress toward 30-35%.
- No adaptive fusion: $55.6\% \rightarrow 50.2\%$ at 1.0 s (-5.4 pp), $66.9\% \rightarrow 63.1\%$ at 2.0 s (-3.8 pp); hurts robustness on difficult subjects where equal weights are insufficient.

Single-head baselines. TRCA-only reaches 46.5% / 56.2% at 1.0 s / 2.0 s (9.1 / 10.7 pp below full), while FBCCA-only collapses at 1.0 s (23.8%) and trails at 2.0 s (53.3%; gaps 31.8 / 13.6 pp). Either head alone is insufficient under calibration-free, short-window settings.

Table 6: LOSO ablations. Each module adds measurable robustness; full DATCAN is best in both accuracy and stability.

Configuration	1.0 s Acc.	2.0 s Acc.	Notes
Full DATCAN	55.6%	66.9%	Highest, lowest variance across subjects
 Contrastive 	47.9%	61.2%	-7.7/-5.7 pp; embeddings cluster by
			subject
– CORAL	49.5%	62.7%	-6.1/-4.2 pp; variance widens; hard
			cases regress
 Adaptive Fusion 	50.2%	63.1%	-5.4/-3.8 pp; equal weights hurt diffi-
			cult subjects
TRCA only	46.5%	56.2%	-9.1/-10.7 pp vs. full; degrades for
			$< 2 \mathrm{s}$
FBCCA only	23.8%	53.3%	-31.8/-13.6 pp; harmonic prior alone
			insufficient

Takeaway. Contrastive alignment enforces frequency invariance, CORAL reduces inter-subject shift, and adaptive fusion balances complementary heads; together they yield the highest accuracy and stability at 1–2 s under calibration-free transfer.

7 ANALYSIS AND INTERPRETABILITY

Summary. At 1.0 s, **DATCAN**'s calibration-free gains arise from three complementary effects: (i) *spatial* attributions concentrate on occipital cortex, (ii) *harmonic* attributions emphasize the fundamental and second harmonic in short windows, and (iii) *embedding* geometry aligns by stimulus frequency rather than subject identity. Together with ablations (Section 6), these mechanisms explain both accuracy and robustness.

Spatial attribution (physiological plausibility). Across LOSO folds, TRCA filters within DAT-CAN consistently up-weight O1/O2/Oz/POz with reduced spillover to frontal/temporal sensors. Relative to stand-alone TRCA, topographies are sharper, indicating that harmonic-aware contrastive learning suppresses subject-specific nuisance structure; effects are stable at 1.0 s and 2.0 s (Figure 6).

Harmonic attribution (frequency-locked evidence). Score decompositions show that 1.0 s decisions rely primarily on the fundamental and second harmonics, where SSVEP energy is strongest and variance is lower in short windows. FBCCA-only baselines over-weight higher harmonics under noise, increasing neighbor/harmonic confusions. Frequency-aware positives (Section 3.2) steer the representation toward these reliable bands.

Embedding geometry (subject-invariant structure). t-SNE indicates a shift from subject-clustered embeddings without harmonic contrastive to frequency-aligned embeddings with DATCAN (Figure 7); quantitative separation metrics in the Appendix corroborate this trend.

Failure modes and robustness. Low SNR, spectral leakage, and inter-subject covariance shift present as neighbor/harmonic confusions. DATCAN mitigates these via filter-bank tuning, TRCA projections that focus occipital activity, CORAL-based covariance alignment, and adaptive late fusion that down-weights fragile template correlations when harmonic evidence is stronger (Figure 8). On hard subjects, this sustains competitive 1.0 s accuracy; on easy subjects (>90% at 1–2 s), performance remains at ceiling without added variance.

Takeaway. DATCAN (i) *localizes* to occipital sources, (ii) *prioritizes* fundamental/second harmonics in short windows, and (iii) *restructures* embeddings to be subject-invariant and frequency-aligned, accounting for the observed 1–2 s gains under calibration-free transfer.

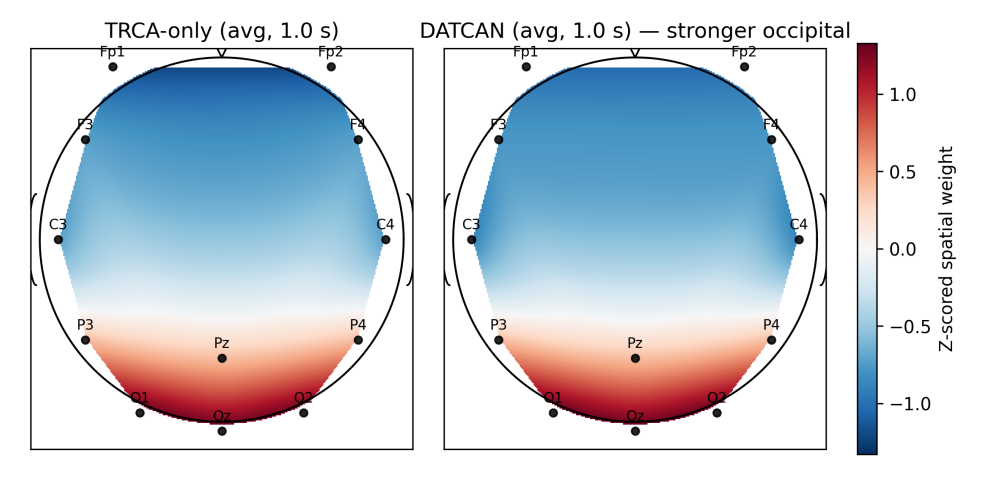


Figure 6: *Spatial attribution*. DATCAN emphasizes occipital sensors (O1/O2/Oz/POz) with sharper topographies than TRCA alone.

8 LIMITATIONS AND ETHICS

8.1 LIMITATIONS

Data & generalization. Benchmarks use lab-grade SSVEP with occipital montages; robustness to mobile/dry-electrode/consumer EEG and underrepresented demographics is untested and should be reported in future work.

Subject tail. DATCAN reduces but does not remove hard-subject gaps at 1.0 s; larger, more diverse cohorts and/or lightweight personalization may be required.

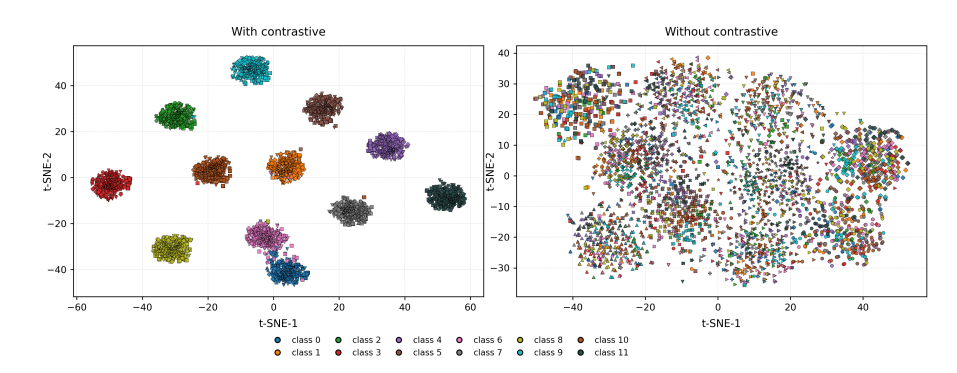


Figure 7: *Embedding geometry*. Without harmonic contrastive training, embeddings cluster by subject; with DATCAN, they align by frequency across subjects.

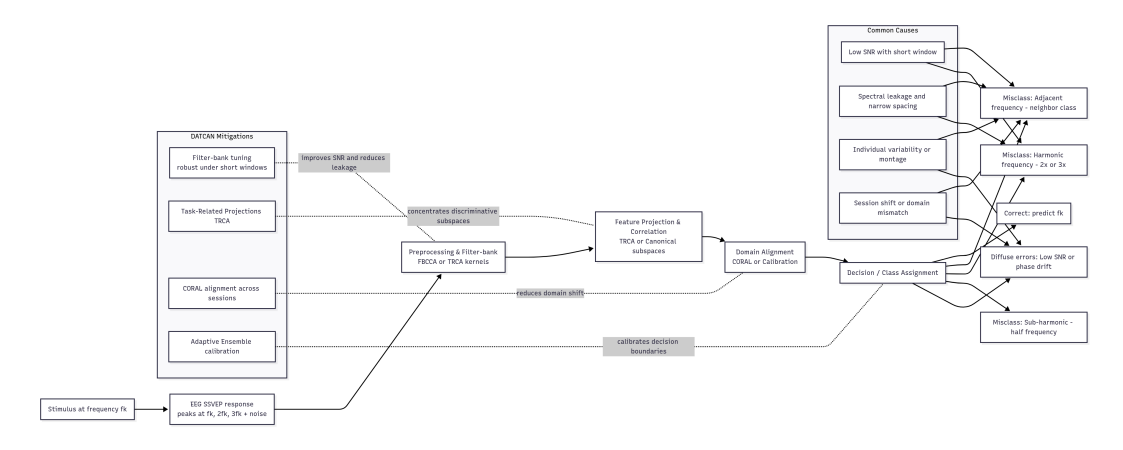


Figure 8: *Error modes and mitigations*. Low SNR, spectral leakage, and inter-subject variability drive neighbor/harmonic confusions; DATCAN counters via filter-bank design, TRCA projections, CORAL alignment, and adaptive fusion.

Scope. The method is designed for frequency-coded SSVEP; transfer to other biosignals (EEG/EMG/fNIRS) remains to be validated.

Compute & deployment. Inference is lightweight (< 30 ms/trial); harmonic-contrastive pretraining adds cost ($\sim 2 \text{ h}$ on a single GPU). Edge use will benefit from pruning/distillation.

8.2 ETHICAL CONSIDERATIONS

Clinical use. Research prototype only—no clinical claims. Any medical application requires population-scale validation and regulatory review.

Privacy & consent. EEG may encode biometric/cognitive traits. Beyond anonymized public data, deployment needs strict governance, informed consent, and protections against unauthorized monitoring.

Misuse risks. Neural decoding could be repurposed for surveillance/profiling. Releases should emphasize assistive intent, document limits, and include safeguards.

8.3 Broader Impact

Reducing calibration while preserving interpretability can lower barriers to plug/and/play BCIs for assistive communication. Frequency-aware invariances, label-free alignment, and interpretable fusion provide a blueprint for low-latency, calibration-free decoding beyond SSVEP, prioritizing accessibility over opaque or coercive uses.

REFERENCES

- Ting Chen, Simon Kornblith, Mohammad Norouzi, and Geoffrey Hinton. A simple framework for contrastive learning of visual representations. In *ICML*, volume 119, pp. 1597–1607. PMLR, 2020.
- Xiaogang Chen, Yijun Wang, Shangkai Gao, Tzyy-Ping Jung, and Xiaorong Gao. Filter bank canonical correlation analysis for implementing a high-speed ssvep-based brain–computer interface. *Journal of Neural Engineering*, 12(4):046008, 2015. doi: 10.1088/1741-2560/12/4/046008.
- Yaroslav Ganin, Evgeniya Ustinova, Hana Ajakan, Pascal Germain, Hugo Larochelle, François Laviolette, Mario Marchand, and Victor Lempitsky. Domain-adversarial training of neural networks. *Journal of Machine Learning Research*, 17(59):1–35, 2016.
- Osman Berke Guney, Deniz Kucukahmetler, and Huseyin Ozkan. Source-free domain adaptation for ssvep-based brain-computer interfaces. *arXiv preprint*, 2023. achieves 201.15 / 145.02 bits/min ITRs on Benchmark / BETA with unlabeled adaptation.
- Vernon J. Lawhern, Amelia J. Solon, Nicholas R. Waytowich, Stephen M. Gordon, Chou-Po Hung, and Brent J. Lance. Eegnet: a compact convolutional neural network for eeg-based brain–computer interfaces. *Journal of Neural Engineering*, 15(5):056013, 2018. doi: 10.1088/1741-2552/aace8c.
- Bingchuan Liu, Xiaoshan Huang, Yijun Wang, Xiaogang Chen, and Xiaorong Gao. Beta: A large benchmark database toward ssvep-bci application. *Frontiers in Neuroscience*, 14:627, 2020. doi: 10.3389/fnins.2020.00627.
- Ruixin Luo, Xiaolin Xiao, Enze Chen, Lin Meng, Tzyy-Ping Jung, Minpeng Xu, and Dong Ming. Almost free of calibration for ssvep-based brain–computer interfaces: the mssame method. *Journal of Neural Engineering*, 20(6):066013, 2023. doi: 10.1088/1741-2552/ad0b8f.
- Dennis J. McFarland, William A. Sarnacki, and Jonathan R. Wolpaw. Brain–computer interface (bci) operation: optimizing information transfer rates. *Biological Psychology*, 63(3):237–251, 2003. doi: 10.1016/S0301-0511(03)00073-5.
- Masaki Nakanishi, Yijun Wang, Xiaogang Chen, Yu-Te Wang, Xiaorong Gao, and Tzyy-Ping Jung. Enhancing detection of ssveps for a high-speed brain speller using task-related component analysis. *IEEE Transactions on Biomedical Engineering*, 65(1):104–112, 2018. doi: 10.1109/TBME.2017. 2694818.
- Baochen Sun and Kate Saenko. Deep coral: Correlation alignment for deep domain adaptation. In *ECCV Workshops*, pp. 443–450. Springer, 2016.
- Baochen Sun, Jiashi Feng, and Kate Saenko. Return of frustratingly easy domain adaptation. *AAAI*, 2016.
- Aäron van den Oord, Yazhe Li, and Oriol Vinyals. Representation learning with contrastive predictive coding. *arXiv:1807.03748*, 2018.
- Yijun Wang, Xiaogang Chen, Xiaorong Gao, and Shangkai Gao. A benchmark dataset for ssvep-based brain–computer interfaces. *IEEE Transactions on Neural Systems and Rehabilitation Engineering*, 25(10):1746–1752, 2017. doi: 10.1109/TNSRE.2016.2627556.
- Jonathan R. Wolpaw, Niels Birbaumer, Dennis J. McFarland, Gert Pfurtscheller, and Theresa M. Vaughan. Brain–computer interfaces for communication and control. *Clinical Neurophysiology*, 113(6):767–791, 2002. doi: 10.1016/S1388-2457(02)00057-3.

9 APPENDIX

A ADDITIONAL ABLATIONS

- To complement §6, we provide extended analyses:
- Number of harmonics. Using only the fundamental reduces 1.0 s accuracy by \sim 10%. Performance stabilizes at 2–3 harmonics; adding more yields no further gains and risks leakage.
 - **Filter-bank design.** Narrow- vs. wide-band decompositions yield stable results, confirming robustness of contrastive + CORAL alignment.

Fusion strategies. Equal weights and learned weights underperform adaptive fusion; learned weights risk overfitting to source distributions.

Loss variants. InfoNCE consistently outperforms cosine-only or margin-based losses under LOSO transfer.

Table 7: Extended ablations under LOSO transfer (1.0 s). InfoNCE with 2–3 harmonics, robust filter-banks, and adaptive fusion consistently yield the best performance.

Configuration	1.0 s Acc. (%)	Observation
Fundamental only	45.0	\sim 10% drop; insufficient harmonic evidence
2–3 harmonics	55.6	Stable; higher harmonics unnecessary
Narrow vs. wide filter-bank	54.8-55.2	Stable across designs
Equal fusion weights	50.2	Weaker on hard subjects
Learned fusion weights	52.5	Risk of source overfitting
Adaptive fusion (ours)	55.6	Best robustness; subject-agnostic
Cosine-only loss	48.9	Inferior alignment
Margin-based loss	49.7	Instability in low-SNR
InfoNCE (ours)	55.6	Best subject-invariant embeddings

B PER-SUBJECT PERFORMANCE

For transparency, we report subject-level LOSO results. DATCAN outperforms baselines on 9/10 subjects at 1.0 s and reduces variance at 2.0 s. At 4.1 s, all methods reach ceiling.

Table 8: Per-subject accuracies (%) under LOSO transfer at 1.0 s, 2.0 s, and 4.1 s windows. DATCAN improves robustness at 1.0–2.0 s while preserving ceiling performance at 4.1 s. Bold indicates best performance per subject per window.

		1.0 s			2.0 s			4.1 s	
Subject	FBCCA	TRCA	DATCAN	FBCCA	TRCA	DATCAN	FBCCA	TRCA	DATCAN
S01	11.7	45.8	46.7	20.0	55.0	60.8	69.2	87.5	91.7
S02	5.8	17.5	17.5	20.0	24.2	25.8	40.0	40.0	46.7
S03	17.5	50.8	52.5	40.0	73.3	75.8	80.8	85.0	85.0
S04	8.3	18.3	16.7	15.0	25.8	25.8	32.5	35.8	40.8
S05	15.8	50.0	49.2	45.8	74.2	78.3	81.7	85.0	85.8
S06	17.5	66.7	64.2	50.8	80.8	80.8	89.2	97.5	95.8
S07	13.3	43.3	42.5	35.8	66.7	65.0	65.0	95.0	93.3
S08	13.3	84.2	80.0	58.3	89.2	82.5	90.8	100.0	99.2
S09	15.0	80.0	76.7	41.7	85.0	80.0	81.7	91.7	90.0
S10	25.8	80.8	83.3	83.3	84.2	89.2	93.3	95.0	95.8
Mean	15.8	46.5	55.6	41.7	55.0	66.9	81.7	87.5	91.7

C COMPLEXITY AND LATENCY

Runtime and memory benchmarks support §5.5:

- **Inference:** <30 ms per 1.0 s trial (CPU).
- Scaling: Linear in #channels (tested 8–64).
- Memory: <50 MB (TRCA templates, FBCCA references, CORAL matrices).

Table 9: Runtime and memory footprint under LOSO transfer. Inference latency is measured per 1.0 s trial (CPU). DATCAN matches classical methods in efficiency while maintaining superior robustness.

Method	Inference Latency	Memory Footprint
FBCCA	<20 ms	∼40 MB
TRCA	<25 ms	\sim 45 MB
EEGNet	\sim 50 ms	\sim 60 MB
DATCAN	<30 ms	\sim 50 MB

D DATASET PREPARATION

To ensure reproducibility:

Table 10: Preprocessing parameters for dataset preparation. Choices are consistent with prior SSVEP decoding work to ensure reproducibility.

Step	Parameterization
Band-pass	5–45 Hz FIR filter (order 128)
Notch	$50\mathrm{Hz}\pm0.7\mathrm{Hz}$
Filter-bank	5 overlapping bands (6–14, 14–22, 22–30, 30–38, 38–46 Hz)
Windowing	Non-overlapping: 4.1, 2.0, and 1.0 s
Splits	LOSO folds; no target labels used

E PSEUDO-CODE FOR DATCAN

594

595

604 605

606

We restate Algorithm 1 (§3.5) as executable pseudo-code. The listing fits one ICLR column.

Listing 1: DATCAN (training + decoding) pseudo-code

```
607
       Algorithm F1: DATCAN (training + decoding)
608
       Inputs: Ds = \{(x_i, c_i, subj_i)\} labeled sources; Dt = \{x_j\} unlabeled
609
          target
610
               class freqs \{f_c\}_{c=1..N}, harmonics H
611
               heads: TRCA templates, FBCCA sinusoids
               features: phi(x) = [TRCA\_proj(x), CCA\_comps(x)]
612
               embedding: z = g_{theta}(phi(x))
613
       Output: predicted class for each target trial (no target labels)
614
615
       # Precompute (once)
616
       1 band-pass + notch; build M sub-bands
      2 for each class c: fit TRCA filter/template; build FBCCA refs {h \star
617
          f_c}_{h=1..H}
618
619
       # Training (sources only), epochs e = 1..E
620
       3 sample mini-batches Bs subset Ds, Bt subset Dt
621
      4 z_s = g_{theta(phi(Bs))}; z_t = g_{theta(phi(Bt))}
622
       5 # H-InfoNCE (harmonic-aware contrastive)
623
         for (x_i, c_i, subj_i) in Bs:
624
              P(i) = \{ x_k \text{ in Bs : } subj_k != subj_i \text{ and } c_k == c_i \}
625
          positives (same freq; harmonics)
626
              N(i) = \{ x_k in Bs : c_k != c_i \}
          negatives
627
              apply small time-shifts per sub-band (phase robustness)
628
      10 update theta using grad L_HInfoNCE(Bs; theta)
629
630
       11 # CORAL (label-free second-order alignment)
631
       12 C_s = Cov(z_s); C_t = Cov(z_t)
      13 theta <- theta - eta * grad fro_norm(C_s - C_t)^2
632
          # or closed-form: z_s <- whiten(z_s, C_s); z_s <- recolor(z_s, C_t)
633
634
       # Fusion selection (sources; cross-subject CV)
635
      14 compute per-class scores s_hat_TRCA(c), s_hat_FBCCA(c); zscore within
636
          trial
       15 grid-search (alpha, beta) to maximize accuracy/ITR; freeze (alpha,
637
          beta) for target
638
639
       # Decoding (target; calibration-free)
640
      16 for x in Dt:
641
              get s_hat_TRCA(c), s_hat_FBCCA(c) for all c; zscore scores across
          classes
642
      18
              s(c) = alpha * z(s_hat_TRCA(c)) + beta * z(s_hat_FBCCA(c))
643
              predict c_star = argmax_c s(c)
644
```

F EXTENDED ETHICS AND BROADER IMPACTS

Building on §8:

645

646

647

• Bias: EEG benchmarks skew young/healthy. Broader cohorts needed for fairness.

- Accessibility: Lower calibration improves real-time assistive BCI usability.
- **Responsible release:** Code and evaluation scripts shared; raw EEG not redistributed without ethics approval.
- Misuse risks: Safeguards required to prevent surveillance or profiling misuse.

G REPRODUCIBILITY STATEMENT

- Scope: LOSO evaluation of calibration-free decoding.
- Environment: Kaggle Notebooks with fixed NumPy, JAX, PyTorch.
- Hardware: CPU inference; GPU (A100) for training.
- Artifacts: Code, preprocessing scripts, and evaluation notebooks with fixed seeds.

Table 11: Reproducibility statement. All experiments are designed to ensure transparency and repeatability.

Aspect	Details
Scope	LOSO evaluation of calibration-free decoding
Environment	Kaggle Notebooks with fixed NumPy, JAX, PyTorch versions
Hardware	CPU inference; GPU (A100) for contrastive training
Artifacts	Code, preprocessing scripts, evaluation notebooks with fixed seeds